Journal of the Korean Nuclear Society
Volume 32, Number 2, pp.180~190, April 2000

Nonlinear Flexural Analysis of PSC Test Beams in CANDU Nuclear Power Plants

In-Hwan BAE, In-Kil CHOI, and Jeong-Moon SEO
Korea Atomic Energy Research Institute
150 Dukjin-dong Yusong-gu, Taejon 305-353, Korea

(Received Nobember 8, 1999)

Abstract

In this study, nonlinear analyses of prestressed concrete(PSC) test beams for inservice inspection of prestressed concrete containments for CANDU nuclear power plants are presented. In the analysis the material nonlinearities of concrete, rebar and prestressing steel are used. To reduce the numerical instability with respect to the used finite element mesh size, the tension stiffening effect has been considered. For concrete, the tensile stress-strain relationship derived from tests is modified and the stress-strain curve of rebar is assumed as a simple bilinear model. The stress-strain curve of prestressing steel is applied as a multilinear curve with the first straight line up to 0.8fpu. To prove the validity of the applied material models, the behavior and strength of the PSC test specimens tested to failure have been evaluated. A reasonable agreement between the experimental results and the predictions is obtained. Parametric studies on the tension stiffening effects, the impact of prestressing losses with time, and the compressive strength of concrete have been conducted.

Key Words : containment, In-Service Inspection(ISI), nonlinear analysis, test beam, material nonlinearity

1. Introduction

Containment design is based on pressure and temperature loadings associated with a loss-of-coolant accident(LOCA)[1]. The containment is also required to protect the internal facilities from external missiles and aircraft impact. Structural integrity is defined as the ability of a structure to withstand the requirements mentioned above[2,3]. The containment building is deteriorated by an effect of environment, crack and disintegration, and structural degradation is occurred in the service life[4].

Most of operating nuclear power plant stations use a prestressed concrete containment(PCC) structures. To investigate the prestressing losses, inservice inspection (ISI) for the prestressing systems in accordance with the regulatory guide has been periodically performed[5].

There are 16 nuclear power plants in operation in Korea. Of the 16 containments, 2 are a steel containment and 14 are prestressed concrete

containments. The prestressed concrete containments consist of 8 unbonded prestressing systems and 6 bonded post-tensioning systems. Evaluation of unbonded prestressing system involves the measurement of tendon forces using the lift-off test for a small random sample. This is a direct approach to estimate the prestressing forces of the tendon at the time of inspection. But the estimation of the bonded prestressing system in containment buildings is based on a series of test beams or pressure test. Construction of the test beams is identical to the containment structure with regard to materials, the amount of reinforcement and the level of prestressing. Wolsung Unit No.1, 2, 3 and 4 in operation are bonded prestressing systems. Prestressed concrete(PSC) test beams are fabricated and evaluated in accordance with the requirement of CSA N287.7 at the period of inspection[6]. The evaluation is accomplished by : (a) a destruction test of the test beams, (b) a series of flexural tests, and (c) a series of lift-off tests[7]. In a technical specification, the analysis procedure to predict the failure loads of PSC test beams is suggested. However, it is found that the method is inadequate because there is a poor correlation between the test results and the calculations. Up to now the analytical study of the PSC test beams reflecting the effects of material nonlinearities and prestressing losses is insufficient[8].

In this study, therefore, a nonlinear analysis with various parameters for PSC test beams, which are tested during inservice inspection for Wolsung Unit No.2[9,10], has been conducted. In the analysis, studies on parameters which have an impact on the behavior of the test beams are conducted. And the test results used to compare with the predictions are from the reports of the 2nd year ISI of Wolsung Unit No. 2 [9,10].

2. PSC Test Beams

2.1. Fabrication of the PSC Test Beams

Construction of the PSC test beams in Wolsung Unit No.2 is identical to the containment structure with regard to the materials used, the level of prestressing, and the percentage of non-prestressed reinforcement[9]. A total of 18 PSC test beams in accordance with the technical specification are fabricated. Of 18 test specimens, 14 beams are completed with bonded tendons and 4 specimens are unbonded prestressing systems. The test beams are prepared in the same manner with each construction stage being carried out at the same time. The placing of the concrete and the stressing of the tendon of the test beams are done at the same time as in the containment structure. The test beams are placed on the plan site and have undergone the same environmental condition as the containment building. The pre-operational proof test of the containment structure is performed at 3 years after its construction and the destruction tests of the test beams are carried out during the 1st and 2nd year ISI thereafter.

2.2. Details of PSC Test Beams

As shown in Figure 1(a), dimension of PSC test

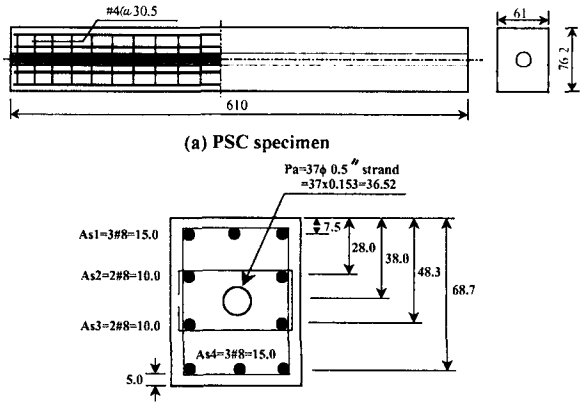

Fig.1. Details of the Test Beams[unit:cm]

beams is 0.61m(W)×0.762 m(H)×6.1m(L). In Figure 1(b), strands(37ϕ0.5″) are used and amount of non- prestressing reinforcement is 50 cm^2. Stirrups at equal spacing are provided to prevent shear failure during the tests. The thickness of the concrete cover is 5 cm.

2.3. Material Properties

2.3.1. Concrete and Rebar

The compressive strength of concrete at the 28th day is 36 MPa and the modulus of elasticity is 28.1 GPa.

The compressive strength and the modulus of elasticity of concrete predicted during the ISI are shown in Table 1. The compressive strength and the modulus of elasticity increase to 24% and 12% compared with that of the design value, respectively. The yield strength and the modulus of elasticity of the rebar are 400MPa and 200 GPa, respectively.

Table 1. Material Properties of Concrete

Period (Year)	Compressive strength fck (MPa)	Modulus of elasticity Ec(GPa)
1 st	42.3 (1.18)	30.5 (1.09)
2 nd	44.5 (1.24)	31.4 (1.12)

( ) : the ratio of the predicted values to the design value

2.3.2. Tendon

The tendon used in containment structures and PSC test beams is 37-0.5″ϕ strands and made in accordance with ASTM A-416. The specified minimum tensile strength and the modulus of elasticity of prestressing steel are 1,860 MPa and 190 GPa, respectively. The total area of the tendon is taken as 3652 mm^2.

Table 2. Material Properties of Used Tendons

Period	Ultimate tensile strength f_{pu} [KN]	0.2% offset load $f_{0.2}$ [KN]	Elongation at failure ε_{pu} [%]
1 st	188.4	180.4	7.42
2 nd	197.2	169.4	6.88

The tendon should be tested up to failure in accordance with KSD 7002-95:tensile load, 0.2% offset load, and elongation at failure of tendon must exceed 183.7 KN, 165.3 KN, and 3.5 %, respectively. Tests for 18 strands during the ISI are performed and the results of the tests are such as shown in Table 2. It is found that all strands do satisfy the requirement of the strandard.

Initial prestressing force is obtained from the results of lift-off tests for the 4 unbonded test beams. Average initial prestressing force (F_i) is 4544.2 KN as $0.67f_{pu}$ (1244.3MPa). The predicted effective prestressing forces of the tendons are as follows. At the 1st year ISI, effective presstressing force is 3,736KN as 1023MPa ($0.82F_i$). The average prestress based on lift-off test of the 4 unbonded test beams is 1054MPa and is 3% greater than the prediction. The prestressing force of tendon at the 2nd year ISI is 3,705.7KN(1014.7 MPa).

2.4. Test Setup

The loading setup in accordance with CSA N287.7 should be a four-point-load configuration at one-third of the beam length but a three-point-load system is applied as shown in Figure 2[10]. To measure deformation of the specimens, displacement transducers are placed at the midspan and at one-fourth of the beam span. The hydraulic jack and the calibrated load cell is set. Experimental data is continuously

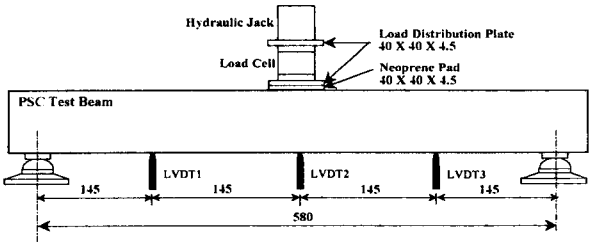

Fig. 2. Test Setup [unit:cm]

recorded from the load cell and displacement transducers.

3. Finite Element Analysis and Results

In this study, the computer program ABAQUS V5.8-9 is used to generate an symmetric model for nonlinear analysis of the PSC test beams. Correlation studies between experimental and analytical results have been conducted to evaluate the validity of the applied material models. Studies on parameters, such as tension stiffening effect, compressive strength of concrete, and prestressing losses have been performed[8].

3.1. Material Models

3.1.1. Concrete

Stress-strain curve for concrete in compression as shown in Figure 3(a) is modified. This model is proposed by Kent and Park and modified by Scott as a confined compressive stress-strain relationship[11]. K is a function of reinforcement ratio (ρ_s) and f_c' is the compressive strength of concrete. To reduce numerical instability with respect to the used finite element mesh size, the tension softening model proposed based on the experimental results is modified as a multilinear model. The two typical stress-strain relations obtained from the test results are as shown in Figure 3(b) [12]. The curve consists of two distinct regions. Before cracking the stress-strain relationship is perfect linear. In the descending

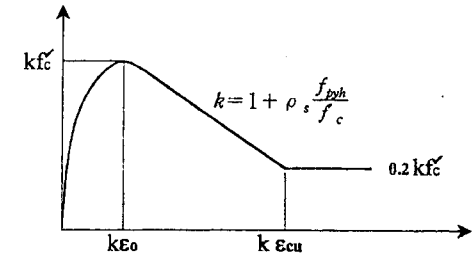

(a) compressive stress-strain curve

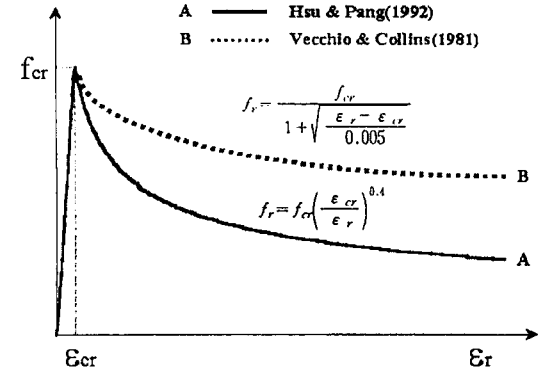

(b) tensile stress-strain curve

Fig. 3. Stress-strain Relations of Concrete

region, the concrete is cracked and the average stress-strain relation becomes concave. The descending equation is proposed by Pang and Hsu(curve A) based on the tests of 35 full-size panels subjected to shear. In this study, eq.(1) of curve A is used for the descending region. And the fracture energy(G_f) of curve B(Vecchio & Collins) is greater than that of curve A (Pang & Hsu). Tension stiffening effect of concrete in tension is considered by using this model.

$$f_r = f_{cr}\left(\frac{\varepsilon_{cr}}{\varepsilon_r}\right)^{0.4} \quad (\varepsilon_r \geq \varepsilon_{cr}) \qquad (1)$$

3.1.2. Rebar and Tendon

The stress-strain curve of a bare bar and that of a steel bar embedded in concrete are quite different. The average stress-strain curve of a steel

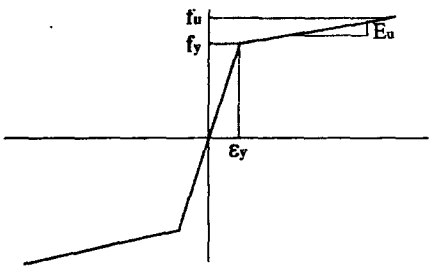

(a) Stress-strain curve of rebar

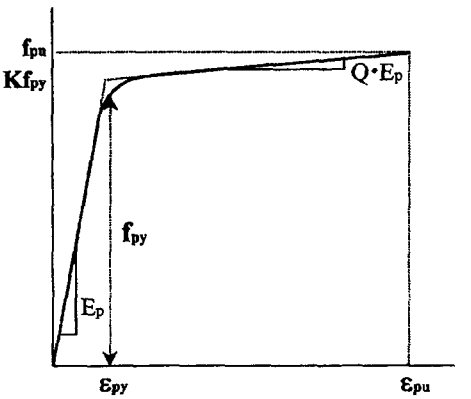

(b) Stress-strain curve of strand

Fig. 4. Stress-strain Relations of the Used Steel

bar embeded in concrete is used. The shape of the average stress-strain relations of mild steel resembles two straight lines with the slope of E_s before yielding and the slope of E_u after yielding. The strain hardening modulus E_u is set to $0.01E_s$. Figure 4(a) shows the average stress-strain relation of a mild steel.

The tensile stress-strain relationship of bare prestressing steel is essentially a curve as shown in Figure 4(b). The curve can be divided into two parts. The first part is a straight line up to $0.8f_{pu}$, where f_{pu} is the ultimate strength of prestressing steel. The second part is expressed by Mattock equation that meets the first part at the stress level of $0.8f_{pu}$. The equation (2) is the applied Mattock equation[13].

$$f_P = \varepsilon_p E_p \left[Q + \frac{1-Q}{(1+\varepsilon^{*R})^{1/R}} \right] \leq f_{pu} \qquad (2)$$

where, $\varepsilon^* = \frac{\varepsilon_p E_p}{K f_{pu}}$, $Q = \frac{f_{pu} - K f_{py}}{\varepsilon_{pu} - E_p - K\varepsilon_{py}}$, f_{py} is yield stress of strand ($0.8f_{pu}$), K and R are constants based on the tests of strands. Based on the ASTM standard for 270 ksi strand, K and R are 1.04 and 8.449, respectively. The ultimate strain at failure is 0.06.

3.2. Finite Element Modelling

The finite element model of test beam consists of 900 elements and 976 nodes. The concrete beam is modeled with four-node symmetric solid elements as shown in Figure 5. All rebar and tendon are modeled using rebar sub-elements in ABAQUS. Slippage of the tendon within the tendon sheath is ignored. Area of load bearing plate($40 \times 40 \times 4.5$cm) is considered. P_e is the predicted prestressing force at the inspection periods in Table 2 and applied as the initial condition.

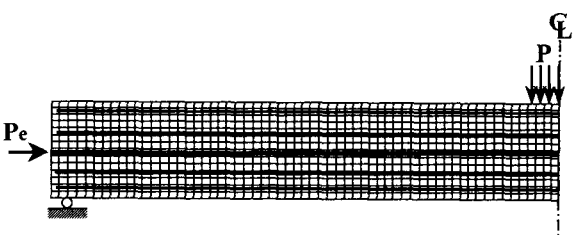

Fig. 5. Modelling of PSC Test Beam

3.3. Results

3.3.1. Crack and Failure Loads

All test beams show the compressive failure of concrete, which is defined as the value of ε_c reaches the ultimate strain ε_{cu} before the yielding of the prestressing steel. Table 3 shows the results of the tests, the numerical results using ABAQUS and the simple calculations according

Table. 3. Results of Experiments, ABAQUS, and Calculations

Period	Items	Experiments [Ref.9, 10]	ABAQUS	Calculations	
				USD	Tech. Spec.[9,10]
1 st Year (Test beam-1)	Cracking loads [KN]	452	429 (0.95)	485 (1.07)	485 (1.07)
	Displ. at cracking [mm]	3.2	4.18 (1.31)	2.9 (0.91)	2.9 (0.91)
	Failure loads [KN]	1432	1444.8 (1.01)	1289.5(0.90)	765.1 (0.53)
	Displ. at failure [mm]	25.4	32.0 (1.25)	-	-
2 nd Year (Test beam-2)	Cracking loads [KN]	468.0	470 (1.01)	492.3 (1.05)	492.3 (1.05)
	Displ. at cracking [mm]	4.19	4.20 (1.01)	2.8 (0.67)	2.8 (0.67)
	Failure loads [KN]	1446.2	1462 (1.01)	1374 (0.95)	1062 (0.73)
	Displ. at failure [mm]	27.5	30.1 (1.09)	-	-

( ) : ratio of ABAQUS and calculations to experiments

to USD and technical specification. In the Table, calculations are determined based on the ultimate strength design(USD) method using the strain compatibility condition and the related technical specification. The compressive failure of concrete is defined as the ultimate compressive strain is reached to 0.004. The ultimate strain ε_{cu} of 0.004 is more realistic than the conservative ACI value of 0.003 [11,12].

For test beam-1, the displacement at cracking of the experiment is 31% greater than that of ABAQUS. For test beam-2, it is found that a reasonable agreement between the experimental results and the ABAQUS results is obtained. It can be found from Table 3 that failure loads obtained from test results agree well with ABAQUS results. The difference between the experiments and the USD is within 10 % but failure loads based on the technical specification are quite different from those of the test results. This is the reason that when it calculates the failure load of the PSC test beam in accordance with the specification, the strength reduction fator, ϕ, for materials is used and thus the ultimate strength of PSC beam is quite underestimated.

3.3.2. Load-midspan Displacement Relationship

The load-midspan displacement relationships obtained from test results are compared with those from ABAQUS. Figure 6 shows the load-midspan displacement relationship of the PSC test beam-1. It is found that initial stiffness(EI_o) of the test result is larger than those of the analytical results, but the behaviors to failure are similar. It is found from Figure 7 that midspan deflections with loading of the test beam-2 agree with those of ABAQUS. Figure 8 shows the load-midspan displacement relationships for all the results. Figure 9 shows load-one fourth span displacement relationships of the test beam-1. It is recognized that the initial stiffness of the test results is slightly greater than that of ABAQUS results. There is a good correlation between the experimental curves and the predicted curves.

3.4. Parametric Study

3.4.1 Tension Stiffening Effect

Based on the fracture energy(G_f), studies on

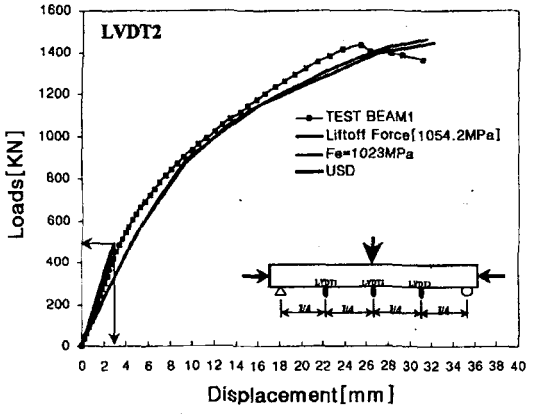

Fig. 6. Load-midspan Displacement Relationship [Test beam-1]

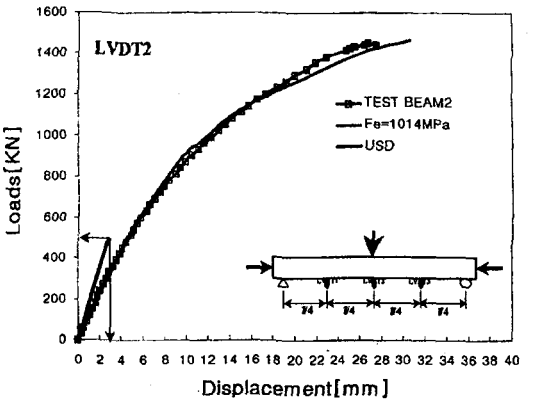

Fig. 7. Load-midspan Displacement Relationship [Test beam-2]

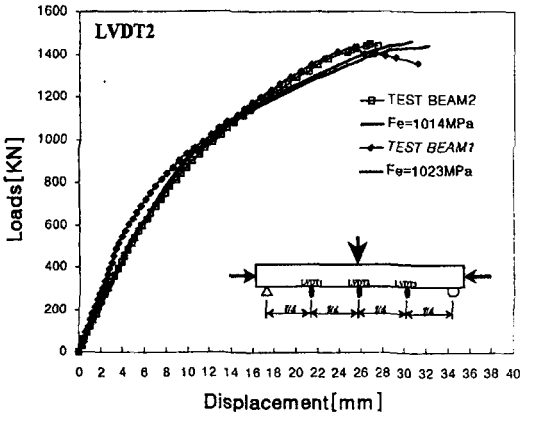

Fig. 8. Load-midspan Displacement Relationship [all beams]

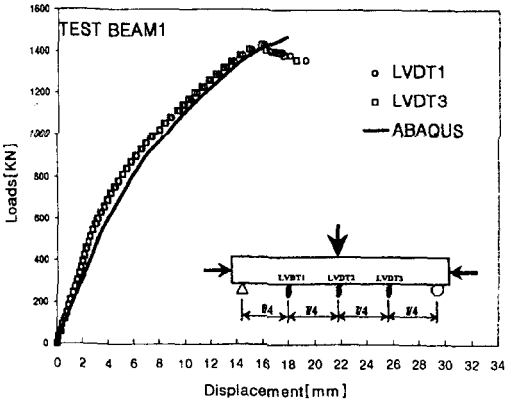

Fig. 9. Load-quater Span Displacement Relationship [Test beam-1]

the behaviors of the PSC test beams by the tension softening models of concrete are conducted. Based on the experimental results of Welch and Heisman(1969), G_f/f_t is the range of 0.005 to 0.01mm and G_f can be determined effectively as a material constant, while f_t is the tensile strength of concrete. The applied tension softening models are bilinear curves and experimental equation(Hsu and Pang,1992). As shown in Figure 10, G_f / f_t is 0.0063mm($\epsilon_0 = 10\epsilon_{cr}$) and 0.027mm($\epsilon_0 = 40\epsilon_{cr}$) for bilinear curves, respectively. The value is 0.012mm for the experimental equation. ϵ_0 is the strain when the tensile stress is zero and ϵ_{cr} is the strain at the tensile strength. The compressive strength of concrete(f_{ck}) and effective prestress(P_e) used for analysis is 454 MPa and 1014.7 MPa, respectively. Figure 10 shows the load-midspan displacement curves with the tension softening models.

The iterative procedure in the ABAQUS program failed to converge for the bilinear models when tensile strain reached to ϵ_0, but in Hsu's model such a numerical problem has not

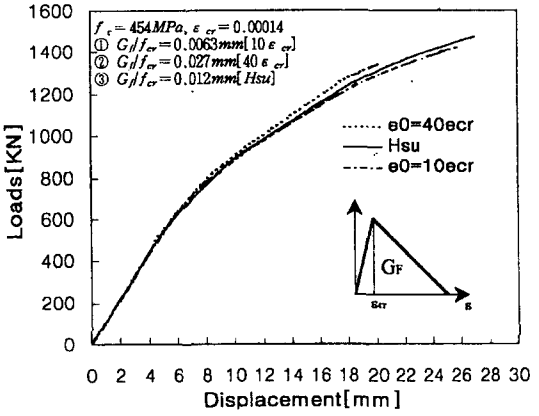

Fig. 10. Load-displacement Curves with Tension Softening Models

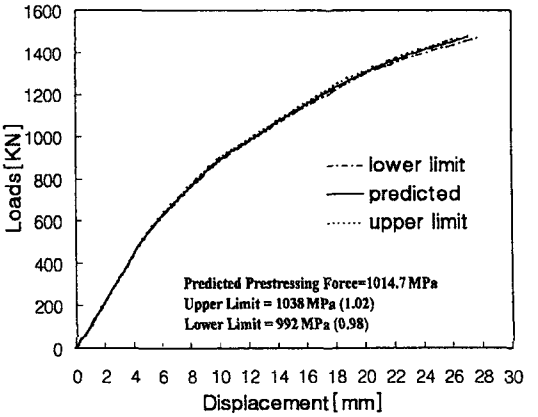

Fig. 11. Load-displacement Curves with Tolerance Band of Acceptable Prestress

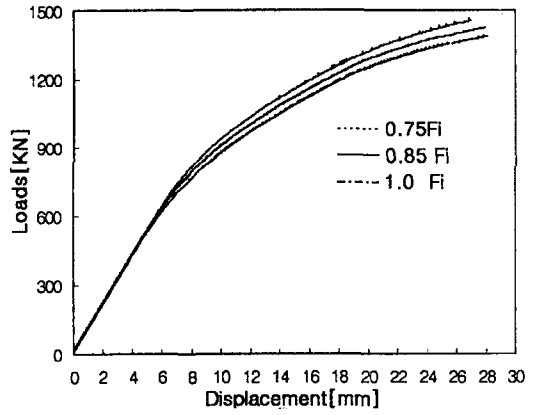

Fig. 12. Load-displacement Curves with Prestressing Losses

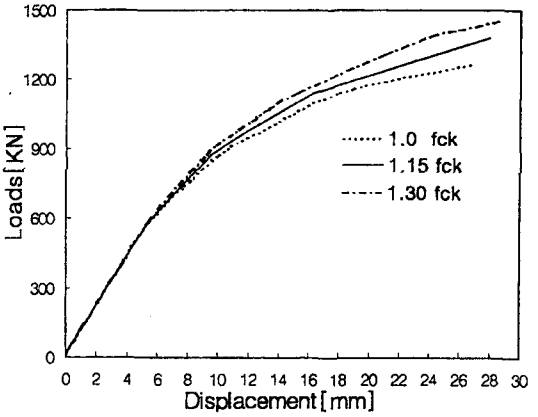

Fig. 13. Load-displacement Curves with Compressive Strength of Concrete

taken place. And it is found that Hsu' s model is adequate to predict the behavior of the PSC test beam.

3.4.2. Effective Prestress

Figure 11 shows the behaviors of the PSC test beam-2 with the allowance of prestress. Applied prestressing levels are as follows : The effective prestress at the 2nd year ISI is 1014.7 MPa, the upper limit and lower limit prescribed in accordance with the technical specification is 1038 MPa(1.02) and 992 MPa(0.98), respectively. It is found from Figure 11 that behaviors before cracking for all cases are the same and each of behaviors after cracking is slightly different. Therefore, if effective prestresses of tendons in PSC containment structures are within the tolerance band of acceptable prestress, it can be said that the containment structure designed primarily as an elastic has leak integrity to contain its coolant system from the LOCA.

Figure 12 shows the behaviors of the test

specimen with prestressing losses. The degree of prestress is varied in three levels - 95%, 85%, and 75% of the initial prestressing force F_i (0.7 f_{pu}). Here, the compressive strength of concrete used is 42.3 MPa. Cracking loads and displacement at cracking decrease with the losses of prestressing forces. It is found that the prestressing losses have a large effect on the behaviors after cracking.

4.3.3. Compressive Strength of Concrete

Figure 13 shows the load-displacement curves with variation of the compressive strength of concrete. The compressive strength of concrete is 36 MPa (f_{ck}), 41.3 MPa ($1.15f_{ck}$), and 46.8 MPa ($1.3f_{ck}$), respectively. In general, the flexural rigidity and the ductility of concrete members increased lightly with the increase of the compressive strength of concrete. It is found that the behaviors for all cases before cracking are similar but the load-deflection relations after cracking are influenced by the compressive strength of the concrete.

4.3.4. Initial Cracks

This section is presented to evaluate the effects of prestressing losses and compressive strength of concrete on initial cracks. The initial cracks can be estimated based on the concept of strain energy, which is defined as the energy accumulated between the origin and the deformation at the crack load. Analysis parameter employed in this study is listed in Table 4.

Figure 14 shows the normalized strain energy with the prestressing losses and the compressive strength of concrete. The initial condition is defined as f_{ck} = 36 MPa, and F_e = $0.6f_{pu}$ (1116 MPa) that is the maximum prestress after all prestress losses in design. It is found from Figure 14 that the slope of normalized strain energy with the prestressing losses is varied still more rapidly than that with the compressive strength of concrete. Therefore, it is concluded that the prestressing losses directly affect the strain energy in concrete at the first cracking.

Table 4. Analysis Parameter

Items	Compressive strength	Prestress level
Initial condition	f_{ck}	F_e
Prestressing effect	f_{ck}	F_e, $0.95F_e$, $0.85F_e$, $0.75F_e$
Compressive strength effect	f_{ck}, $1.05f_{ck}$, $1.15f_{ck}$, $1.3f_{ck}$	F_e

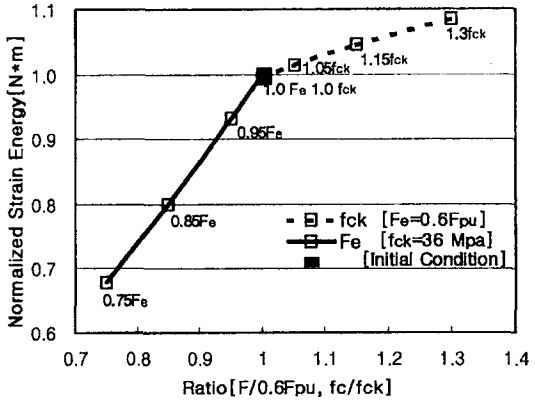

Fig. 14. Normalized Strain Energy with Analysis Parameter

4. Conclusions and Discussion

In this study, nonlinear analyses of PSC test beams using the material nonlinearity have been conducted. The following conclusions are

obtained from this study.

1. Based on above analysis results, material models of concrete and tendons applied are adequate to predict the behaviors of PSC test beams.
2. The present study indicates that there is a good correlation between the test results and the predictions. But the technical specification is inadequate to evaluate the failure loads of the test beams
3. Based on a parametric study, tension softening models and prestressing losses will have direct influence on the behaviors of containment structures. It is concluded that the structural safety and leak integrity of containment structures during the service life may be evaluated by conducting a nonlinear analysis with an adequate material model and effective prestress.

The main function of the containment prestressing system is to counterbalance the tensile stress resulted from a loss of coolant accident(LOCA). Flexural testing of PSC test beams is indirect method of evaluation for structural integrity and its results do not quantify the structural integrity. More studies for these matters are needed.

Acknowledgements

This Project has been carried out under the Nuclear R&D Program by MOST.

References

1. CSA Standard CAN3-N287.7-M82,"Design Requirements for Concrete Containment Structures for CANDU Nuclear Power Plants," Dec., (1982).
2. Choun,Y.S.,and Lee,H.P.," Structural Behavior of Aged Containment Building under Internal Pressure", Proceedings of the Korean Society of Civil Engineers, Vol(I), Seoul, Korea, pp.583~590, Oct. (1998).
3. KAERI, "Development of Integrated Nuclear Safety Assessment Technology, KAERI/PR-/98, (1893).
4. Choun,Y.S.,and Lee,H.P.," Nonlinear Behavior of a Prestressed Concrete Containment Building with Material Degradation," Proceedings of the Korean Nuclear Society Spring Meeting, Seoul, Korea, May, (1999).
5. Ashar, H., and Jeng, D., "Effectiveness of Inservice Inspection Requirements of Prestressed Concrete Containments-U.S.Experience,, Int'l Conf. on containment design and operation, (1990).
6. CSA Standard CAN3-N287.7-M80,"In-Service Examination and Testing Requirements for Concrete Containment Structures for CANDU Nuclear Power Plants," April, (1980).
7. Pandey, M.D., "Reliability-Based Inspection of Prestressed Concrete Containment Structures," AECE Project, No.2.247.3, Canada, March, (1996).
8. Bae, I.H., Choi,I.K. and Seo,J.M.,"Nonlinear Analysis of PSC Test Beams in CANDU Nuclear Power Plants," Proceedings of the Korean Nuclear Society Spring Meeting, Seoul, Korea, Oct, (1999).
9. KOPEC,"The 1st Year In-Service Inspection of Wolsung N.P.P Unit 2 Containment Building Post-Tensioning System", June, (1998).
10. KOPEC, "Report for 2nd In-Service Inspection of Wolsung N.P.P Unit 2 Containment Building Post-Tensioning System," Dec, (1998).

11. Scott, B.D., Park, R., and Priestley, M.J.N., "Stress-Strain Behavior of Concrete Confined by Overlapping Hoops at Low and High Strain Rates", ACI, Vol.79, No.1, pp.13~27, (1982).
12. Hsu,T.C.,"Unified Theory of Reinforced Concrete," CRC, pp.204~205
13. Mattock,A.H.,"Modification of ACI Code Equation for Stress in Bonded Prestressed Reinforcement at Flexural Ultimate," ACI Journal, Proceedings, Vol.82,No.4, pp.331 ~339, July-Aug.,(1984).